RADIATION DOSE MEASUREMENTS AND A STUDY OF DAMAGE TO ACCELERATOR COMPONENTS IN THE TRISTAN e^+e^- COLLIDER AT 27.5 GeV

T. Momose, H.Hirayama,T.Ieiri, K.Takayama, Y.Ohsawa,K.Endo,H.Ishimaru,Y.Mizumachi, S.Takeda, T.Kawamoto and K.Uchino
National Laboratory for High Energy Physics, 1-1 Oho, Tsukuba-shi, Ibaraki-ken, 305, Japan

Abstract

The TRISTAN e^+e^- collider has been operated at a beam energy of 27.5 GeV, with a characteristic energy of the synchrotron radiation of 187 keV. The radiation in the TRISTAN tunnel was measured using thermoluminescence dosimeters.

The dose distribution in the arc sections is influenced by the iron yoke and by gaps in the lead shields. The dose rate on the aluminum chamber surface is about 10^6 Gy/Ah, where 1 Ah accumulates in about 10 days of operation. A 10mm lead shield reduces the dose rate to 10^4 to 10^5 Gy/Ah. The dose rate at shielding gaps reaches 10^5 Gy/Ah. Lead shields of 5 mm thickness reduce the dose rate by a factor of 20 to 80.

Radiation damage to the aluminum vacuum system is mainly from HNO_3, produced from NO_x. Connectors of distributed ion pumps and cables of beam position monitors were damaged by fluorine gas, resulting from the decomposition of Teflon insulators in cables and connectors. Reading and writing functions of 64 kbit RAM's and EPROM's were lost at 700 Gy. Operational amplifiers broke at $3x10^4$ Gy. Nitril-Butadiene rubber hoses for magnet cooling water were hardened by a radiation dose of $2x10^5$ Gy. Magnet coils have survived 10^6 to 10^7 Gy.

When the beam energy was raised from 25 to 27.5 GeV, the dose rate doubled in the straight sections, while increasing five-fold at the center of the bending magnets. Therefore tight shielding will be required when the beam energy is raised as planned.

Introduction

The electron(e^-)-positron(e^+) colliding ring, TRISTAN (main ring, TMR) was operated first in October 1986 at a beam energy of 25 GeV. Since then the beam energy was gradually increased to 26.5 GeV(May 1987), 27 GeV (June 1987), 27.5 GeV (October 1987) and 28 GeV(January 1988). The characteristic energy of 187 keV for 27.5 GeV operation is the highest in the world.

As the beam energy and current were increased, radiation damage of accelerator components became increasingly apparent. Therefore the radiation dose distribution was monitored and several methods were applied to control the damage.

This paper describes dose distributions, some examples of radiation damage, and methods to control the damage and corrosion.

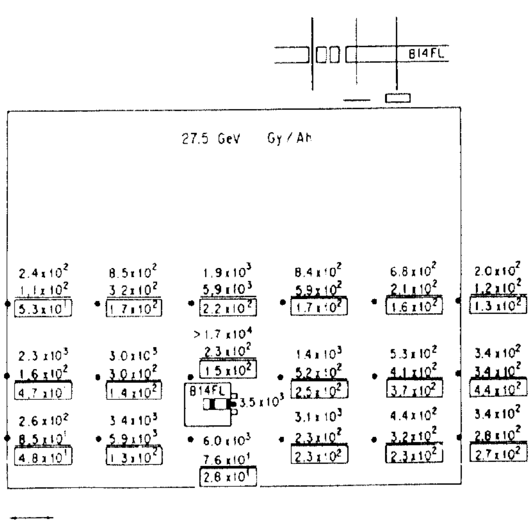

Figure 1 Dose rate distribution over a tunnel cross section at the midpoint of a dipole (□), near the end of a dipole (-) and between the dipole and a quadrupole magnet ( ).

Method of Dose Rate Measurements

All doses were measured with thermoluminescence dosimeters (TLD: BeO [UD-170L]). All doses are quoted as absorbed radiation in air.

The dosimeters were encapsulated with plastic cases to avoid fading due to visible light, and were evenly spaced on strings spanned across the tunnel, and along various components. TLD's were also mounted inside the lead shielding plates to study the attenuation of dose.

Measurements were carried out at 27.5 GeV for both the electron mode and the electron-positron mode. To avoid saturation, the exposure time was limited to 120 seconds. The beam currents were also restricted, to 0.33 mA for electrons only, and to 0.5 mA for the electron -positron mode. The contribution of high energy electrons to the total dose can be neglected because the beam loss during the exposure is negligibly small, except near the beam stopper.

All measurements are normalized to a dose of 1 Ah of circulating beam, either electrons or electrons plus positrons.

Dose Distribution

1. General Character of Dose Distributions

Dose rates for 27.5 GeV operation were:

On the beam chamber surface, without lead shield:	over 10^6 Gy/Ah
Near a gap in the lead shield	~10^5 Gy/Ah
Near the beam chamber, with lead shield:	10^4~10^5 Gy/Ah
Inside the tunnel	10^1~10^4 Gy/Ah

2. Cross-sectional Distribution in the Tunnel

Figure 1 shows the dose rate distribution over a tunnel cross section at the midpoint of a dipole , near the end of a dipole, and between the dipole and a quadrupole magnet. The vacuum chamber inside the dipole magnet was covered with a 2 cm thick lead shield on the outer face, and a 1 cm thick shield on the inner face. The chamber outside the dipole was shielded with 1 cm of lead.

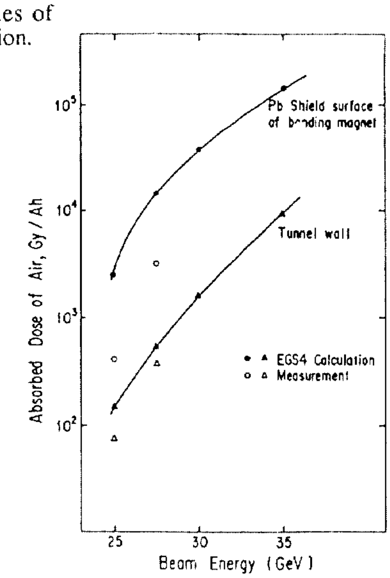

Figure 2 Beam energy dependence of measured and calculated dose rates.

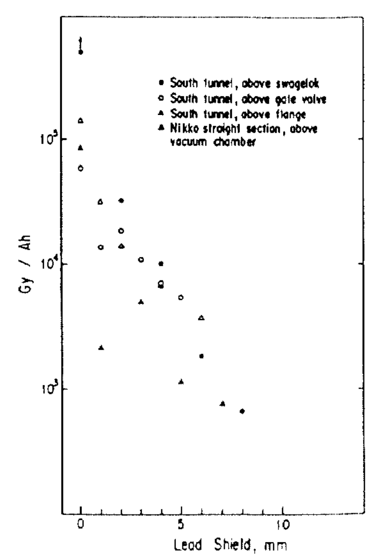

Figure 3 Attenuation of dose rate by lead plates from 1 to 8 mm thick.

The dose distribution for the midpoint of the dipole shows that the photons come mainly from the open side of the magnet yoke, while the area behind the magnet yoke receives only 1/10 the dose, due to the shielding by the iron. The distributions are generally similar to those measured at PETRA[1] except for an increase above the magnet yoke, which may be due to a gap in the shield at the end of the dipole magnets. Between the dipole and the quadrupole magnets, the dose rate increases drastically due to the absence of the iron yoke, especially on the outer side.

The dose measurements were compared to calculations using the EGSA4 Monte Carlo code[2]. Fig. 2 shows the comparison at 25 GeV. The calculated dose rates exceed the measured ones by about a factor of 5 at the shield surface of the dipole magnet , but the beam energy dependence is well reproduced. For a beam energy of 35 GeV the calculations predict a dose rate of 3×10^4 Gy/Ah at the shield surface, and 7×10^3 Gy/Ah at the tunnel wall.

3. Dose Rates Within the Lead Shields and in the Straight Sections

For four positions on the vacuum chamber we investigated the attenuation by lead plates from 1 to 8 mm thick. The attenuation curve, shown in Fig. 3, is nearly exponential, showing a decrease by a factor 20 to 80 for a 5 mm lead shield.

Dose rates at 27.5 GeV for the straight section "Nikko-Left" are shown in Fig. 4. For both the chamber surface and the tunnel wall, the dose rate falls exponentially with distance from the arcs. The chamber surface dose shows, however, some sudden peaks, especially behind some quadrupole magnets. Fig. 4 also shows earlier measurements at 25 GeV. The dose at the tunnel wall has doubled when the beam energy was raised.

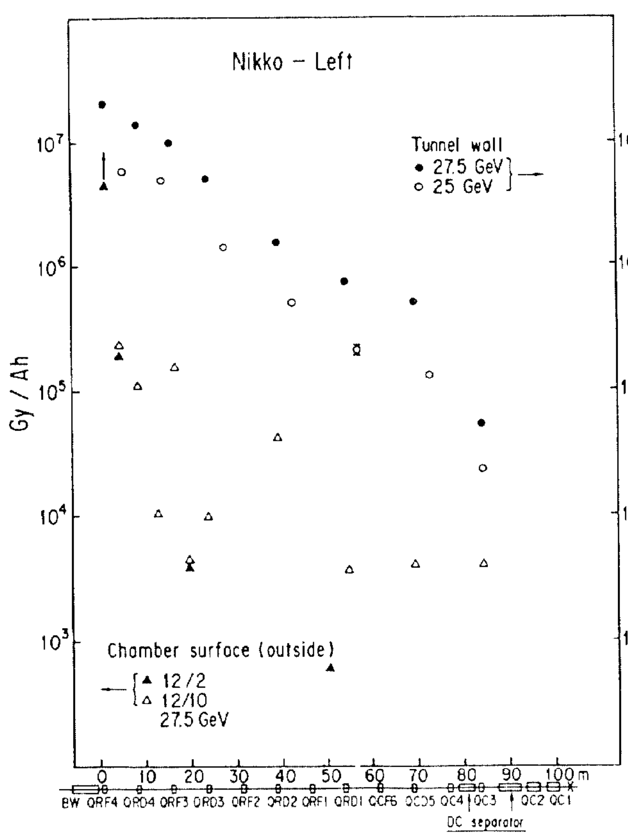

Figure 4 Dose rate at 27.5 GeV for the straight section "Nikko-Left" as a function of distance from the arcs (left side).

Effect of the Synchrotron Radiation on Magnets

As the energy of the TRISTAN main ring is increasing, synchrotron radiation damage is expected. We see already some hardening of the cooling water hoses used on sextupole and wiggler magnets. These hoses are made of Nitril-Butadiene rubber, which has a radiation tolerance of 5×10^5 to 10^7 Gy. Ethylene-Propylene rubber is used for other magnets in the same environment and doesn't show any serious radiation damage yet. The radiation dose rate around the chambers is, from our measurements, in the range 10^4 to 7×10^5 Gy/Ah in the arcs, about 5×10^5 Gy/Ah at the beginning of the detector insertions (following the weak bending magnet) and 1.5×10^6 Gy/Ah at the symmetry point of the arc. Note that 1 Ah of beam integral accumulates during 10 days of normal operation with four bunches at 27.5 GeV. The total accumulated beam integral so far is estimated at more than 10 Ah.

The vacuum chamber in the arc sections is covered with lead shields, but there are many gaps in the shields which allow radiation to escape. A typical example of such radiation leakage is shown in Fig. 5, which was obtained from the exposure of radiation sensitive color sheets ("Radcolor") to 1.5 Ah of beam. In other places, such as the wiggler section and the experimental straight sections, the vacuum chamber is not shielded. Magnet coils have been exposed to up to 1.5×10^7 Gy and suffered serious damage, while other areas receiving 10^5 to 7×10^6 Gy escaped damage. Higher radiation levels are anticipated as both the beam intensity and the machine energy will increase. Unless the radiation attenuation around the machine is improved by two orders of magnitude many components will reach their radiation tolerance limit since the radiation dose appears to increase about tenfold each year.

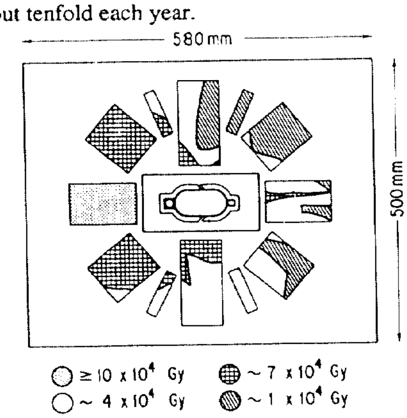

Figure 5 Typical example of radiation leakage between a sextupole and a bending magnet.

The Aluminum Vacuum System and the Beam Position Monitors

The TRISTAN collider consists of an accumulator ring (TAR) and a main ring (TMR), both of which have all-aluminum vacuum systems. Above 6 GeV for TAR and above 15 GeV for TMR the synchrotron radiation is energetic enough to penetrate the aluminum chambers (3mm wall for TAR and 4mm wall for TMR) and interact with materials outside the chamber. Damaged and corroded components of the vacuum system were chemically analysed, with the results shown in Table I and II.

Table I shows the composition of the corroded material falling from the lead shield onto a bellows surface(1), corroded material removed from the anodized surface of bellows (2, 3), from the extruded aluminum chamber (4) and from the lead shield around the bellows(5). The data indicate that NO_x was produced by synchrotron radiation, and combined with water to attack aluminum and lead surfaces. Similar damage from NO_x was also observed on Kapton thermal insulating film, where evaporated aluminum disappeared due to radiation leaking from gaps in the shielding.

It is extremely important to protect the bellows from corrosion. This has been done by eliminating oxygen and water vapor from their surface. Dry Nitrogen gas with a dew point of -70 C is being supplied to all the bellows in TAR and TMR since January 1988. New bellows with ceramic coating[3] were developed and two have been installed in the TMR.

No. Samples	Cl^-	NO_2^-	NO_3^-	Al	Pb
(1) Bellows	—	0.21	7.1	<2.9	56
(2) Bellows	0.13	—	20.0	28.2	<4
(3) Bellows	—	—	20.2	20.2	<11
(4) Al Surface	—	—	22.6	21.9	10.7
(5) Pb Surface	—	0.14	6.4	<0.4	69

(%) (μg)

Table I Composition of the corroded materials.

Samples	F	Cu	Fe	Cr	Ni
Cable	183	180	14	—	—
Connector	249	136	92	22	16

(μg)

Table II Composition of corroded BPM components.

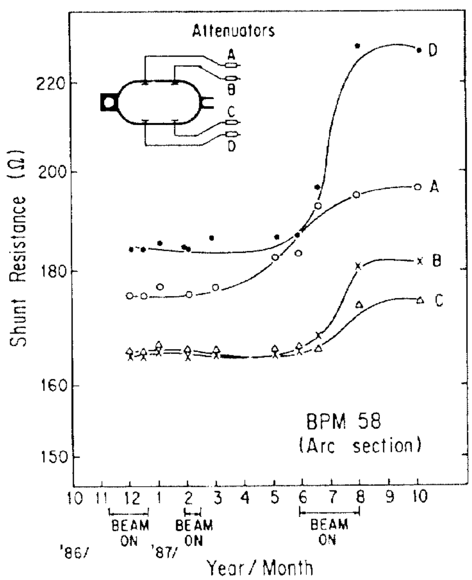

Figure 6 The shunt resistance of an Rf attenuator in an arc section as a function of operating time.

Table II shows analyses of corroded BPM components, where the cables and connectors were insulated with Teflon. Teflon in the cables shrinks under irradiation. Fluorine from the Teflon is also seen to corrode metal parts of cables and connectors. Similar damage is observed on the pins and sockets of DIP's. We are now changing these components over to polystyrene and polyethylene. Connectors with ceramic insulation are also being developed. Rf attenuators used between the BPM's and their cables are also attacked by fluorine gas. The shunt resistance of these attenuators is shown in Fig. 6 as a function of operating time.

No.	Designation		Type	Exposure dose (Gy)				
				Sample 1 5.8×10^2	Sample 2 5.3×10^3	Sample 3 6.7×10^4	Sample 4 2.0×10^5	Sample 5 2.6×10^6
1	Transister	Si, NPN	2SC373-G	—	—	—	—	—
2	〃	Si, 〃	2SC387AG	—	—	—	—	—
3	〃	Si, 〃	2SC780AGY	—	—	—	—	—
4	〃	Si, PNP	2SC495-Y	—	—	—	—	—
5	〃	Si, 〃	2SA499-Y	—	—	—	—	—
6	〃	Si, 〃	2SA504-GR	—	—	—	—	Δ
7	〃	Si, NPN	2SC504-GR	—	—	—	—	—
8	〃	Si, FET, N-channel	3SK28-GK	—	—	—	—	—
9	Integrated	TTL gate	74ALS00AN	—	—	—	—	—
10	〃	〃 inverter	74ALS04A	—	—	Δ	Δ	Δ
11	〃	〃 counter	Am25LS2569PC	—	—	—	—	—
12	〃	CMOS RAM(64k-bit)	HM6264LP-15	—	—	X	X	X
13	〃	CMOS EPROM(64k-bit)	HN27C64G-20	—	—	X	X	X
14	〃	opt. coup. isolator	TIL112	—	—	—	—	—
15	〃	〃 〃 〃	6N 137	—	—	—	—	—
16	〃	CMOS analog mpx.	HI-508A	—	—	Δ	Δ	X
17	〃	op. amplifier, FET input	CA3140E	—	—	Δ	Δ	X
18	Capacitor	Al electrolytic	1μF 50V	—	—	—	—	—
19	〃	tantalum	1μF 35V	—	—	—	—	—
20	〃	〃	6.8μF 35V	—	—	—	—	—
21	〃	ceramic, piled electrode	0.1μF 50V	—	—	—	—	—
22	〃	polyester film	0.1μF 50V	—	—	—	—	—

— : Stable Δ : Damaged X : Broken

Table III Summary of radiation damage to electronic components.

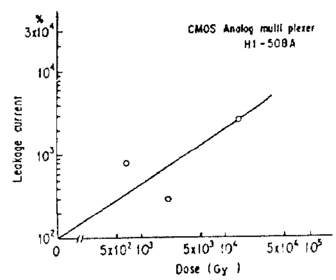

Figure 7 Leakage current of an analog multiplexer as a function of dose.

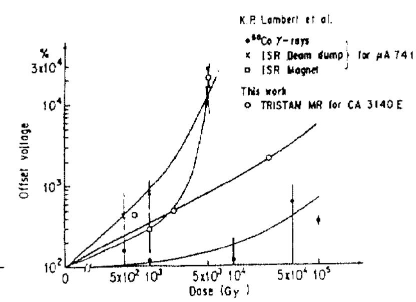

Figure 8 Offset voltage of an operational amplifier as a function of dose.

Electronic Components

Samples of electronic components were placed along the beam chamber while being operated at normal voltage and power levels. Operational amplifiers and transistors were operated as voltage followers. The components received doses of 600 Gy to 2.6 x 10^6 Gy in 5 steps. The results are shown in Table III. We observed that:

1) Reading and writing functions of 64 kbit -RAM and EPROM chips were lost at only 700 Gy.
2) The temperature of a transistor (2SA504-GR, Pc=800mW) rose at 3 x 10^4 Gy, but it continued to function normally.
3) A TTL inverter (74ALS04A) functioned normally, except that V_{OH} became +5V at 700 Gy.
4) The leakage current of an integrated CMOS analog multiplexer (HI-508A), with the gate off, rose at 700 Gy.
5) The offset voltage of an operational amplifier (CA3140E) increased at 700 Gy and the amplifier failed at 3 x 10^4 Gy.

The results are shown in Figs. 7 and 8, together with previously published data[4,5]. Their dose dependence shows different slopes for different incident particles.

Summary

Measurements at TRISTAN at 27.5 GeV show dose rates of 105 Gy near gaps in the lead shielding, and about 106 Gy for an unshielded chamber. Magnet coils in the arc sections have been irradiated with 10^6 to 10^7 Gy so far. These numbers point to the urgent need for tighter radiation shields for all vacuum chambers. Connectors for DIP's and BPM's, Rf attenuators, aluminum bellows, chamber surfaces and gate valves have also been irradiated with about 10^6 Gy. They are damaged by fluorine gas from Teflon insulated cables and connectors, and by HNO_3, made from NOx. To combat corrosion, bellows are being flushed with nitrogen gas, and new ceramic coated bellows are being tested. Some electronic components begin to fail at 100 Gy. For the higher radiation levels anticipated with the higher beam currents and energy planned, tighter radiation shielding is mandatory. The dose distribution must be studied further, and methods for the protection of the accelerator components must be developed.

Acknowledgements

The authors wish to thank Assoc. Prof. M. Kanda and Mr. M. Taira at KEK for their chemical analyses and helpful discussions.

References

1 H. Dinter, Nucl. Instr. and Meth. A239(1985) 597.
2 W. R. Nelson, H. Hirayama and D.W.O. Rogers, SLAC-265 (1985).
3 M. Miyamoto et al., JVST , A4(6), Nov/Dec (1986) 2515.
4 K.P. Lambert et al., A comparison of radiation damage of electronic components irradiated in diffferent radiation fields, CERN 75-4 (1975).
5 S. Battisti et al., Radiation damage to electronic components, CERN 75-18 (1975).